IOSR Journal of Applied Physics (IOSR-JAP)
e-ISSN: 2278-4861.Volume 10, Issue 5 Ver. II (Sep. – Oct. 2018), 15-25
www.iosrjournals.org

Synthesis, Growth, Linear and Nonlinear Optical properties of L-Valine Imidazole: An Organic Nonlinear Optical Single Crystal

K. Lilly Mary Eucharista[a], C. Krishnan [b] and P.Selvarajan[c]
[a]. *Research scholar, Reg.No.8230, S.T.Hindu College, Nagercoil, Affiliated to ManonmaniamSundaranar University, Abishekapatty, Tirunelveli.*
[b.] *Department of Physics, Arignar Anna College, Aralvoymoli-629 301, Tamil Nadu, India.*
[c.] *Department of Physics, Aditanar College of Arts and Science, Tiruchendur-628 216, Tamil Nadu, India.*
Corresponding Author: K. Lilly Mary Eucharista

Abstract:*Growth of L-valine imidazole (LVI) single crystals were grown from aqueous solution by slow evaporation technique. L-valine imidazole salt was synthesized and solubility studies have been carried out by gravimetric method in the temperature range of 30-50 °c. The grown crystals were characterized by x-ray diffraction analyses. The important optical parameters such as absorption coefficient, extinction coefficient, refractive index, optical band gap, optical conductivity and electrical conductivity were estimated fromUV–vis–NIR spectral analysis to study the linear optical behavior of the material. Fourier transform infrared (FTIR) study was used to confirm the presence of various functional groups in the grown crystal. The TG and DTA analyses ensure that the material is thermally stable up to 203 °c. The hardness parameters such as microhardness number, work hardening coefficient, yield strength and elastic stiffness constant of the grown LVI crystals were calculated from microhardness studies. Second harmonic efficiency (SHG) of the grown material is 0.74 times as that of KDPcrystal. The laser damage threshold value of LVI crystal is 11 Gw / cm^2 which is greater than the standard KDP material.The SEM micrograph of LVI indicates that the crystal exhibits the cylindrical shape - like structure with an average particle size of 1-10 μm. Fluorescence spectrum shows that the sharp emission peak occurs at 530 nm.*

Keywords: *Ssolution growth, Optical studies, Mechanical properties, LDT, SHG, Thermal analysis.*

Date of Submission: 17-09-2018 Date of acceptance: 03-10-2018

I. Introduction

The extensive research of new nonlinear material is an important task because of their application in telecommunication for efficient signal processing and optical information storage devices. Organic nonlinear optical materials are of current interest for they are being used in advanced optical data processing devices [1-5]. Organic crystals exhibit higher nonlinear optical efficiency compared to inorganic crystals. The high second harmonic conversion efficiency and transparency in visible, ultraviolet are required for various devices in the field of optoelectronics and photonics. Amino acids are good materials for NLO application because they contain proton donor carboxyl acids (- COO) group and the proton acceptor (NH_2) group. L-Valine is an important amino acid which has been exploited for the formation of salts with different organic acids [6-9]. In the present investigation, a systematic study is carried out on the growth and characterization of L-Valine Imidazole (LVI). An organic nonlinear optical single crystal (L-Valine Imidazole) was grown successfully from aqueous solution by a slow evaporation method. The grown crystal was characterized by single crystal XRD, FTIR, optical studies, thermal analysis, mechanical studies, nonlinear optical properties, laser threshold damage study, fluorescence studies and surface morphology and the results were reported in detail.

II. Synthesis and solubility

The title compound was synthesized by taking AR grade L-Valine and Imidazole in the molar ratio 1:1 by a slow evaporation method. Calculated amounts of the chemicals were dissolved in a solvent and the salt was synthesized and it was re-crystallized twice. The solubility of L-Valine Imidazole in pure deionized water was measured at a constant temperature range from 30 to 50 °C. The solution was continuously stirred to maintain homogeneity. A volume of 10 ml of each solvent was taken in an airtight container. Once supersaturation was attained, the experiment was carried out at various temperatures from 30 to 50 °C. It is observed that LVI exhibits positive solubility temperature gradient and the solubility almost increase linearly with the rise in temperature. This shows the slow evaporation technique is the appropriate method for the growth of LVI crystal. The solubility curve is shown in Fig. 1.

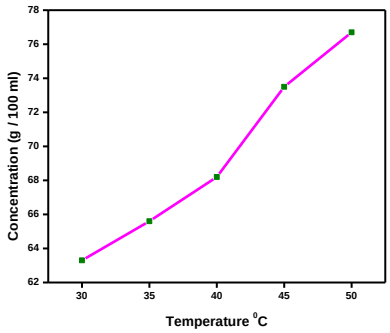

Fig. 1 Solubility curve of LVI crystal

Crystal growth

Single crystals of LVI were grown by solution method with slow solvent evaporation technique at room temperature (30 ^{o}C). In accordance with the solubility data, the saturated solution of the twice re-crystallized salt of LVI was prepared by dissolving the salt in de-ionized water by continuous stirring of the solution and filtered using 4-micron Whatmann filter paper. Then the filtered solution was taken in a beaker and covered by a perforated cover for controlled evaporation. The seed crystals of LVI were obtained by spontaneous nucleation. Two or three good quality seed crystals of LVI were placed in the supersaturated solution and the solution was allowed to evaporate the solvent slowly into the atmosphere. A typical single crystal was obtained within a period of 20 days. The photograph of the grown crystal is displayed in Fig.2. The grown crystals are found to be stable, non-hygroscopic at ambient temperature, transparent and colorless.

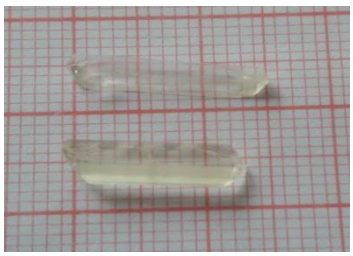

Fig. 2 Photograph of LVI crystal

III. Results and discussion

X-ray diffraction studies

The grown crystals were subjected to single crystal x-ray diffraction analysis using an ENRAF NONIUS CAD-4 single crystal X-ray diffractometer with M_o K_α (λ = 0.7170 Å) radiation to determine the lattice parameters. The calculated lattice parameters are a = 10.43 Å, b = 5.78 Å, c = 11.36 Å,$\alpha = \gamma = 90^o$, β = 119.90^o and volume = 2 34.3(1) Å^3. The crystal belongs to the monoclinic system.

The grown LVI crystals were finely powdered and have been subjected to powder XRD analysis. All the observed reflections were indexed. The well-defined Bragg's peaks at a specific 2θ angles show the good crystallinity nature of the grown crystal. All the observed reflection planes were indexed using TREOR software packages following the procedure of Lipson and Steeple [10]. The indexed powder XRD pattern of the grown crystal is shown in Fig. 3.

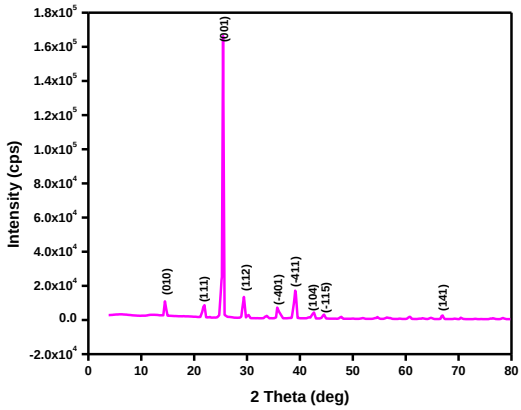

Fig. 3 Powder X-ray diffraction pattern of LVI

FTIR analysis

The functional groups of LVI were confirmed by recording the FTIR spectrum in the range of 4000 - 400 cm^{-1} using KBr pellet technique and the resultant spectrum is shown in Fig. 4. The sharp peak at 3438 cm^{-1} is due to O-H stretching of L-Valine. There are two bands which are identified for the N-H bending vibrations for imidazole in the FTIR spectrum. These are assigned to the band at 3345 cm^{-1} and 1620 cm^{-1}. A weak band at 2820 cm^{-1} and sharp peaks at 1464 cm^{-1}, 639 cm^{-1} are due to C-H bending vibration of alkanes. The weak band at 1676 cm^{-1} is due to C = O stretching vibration of L-Valine. The band at 2209 cm^{-1} and 1136 cm^{-1} are due to C-N stretching vibrations. The weak band at 2131 cm^{-1} is due to C-C stretching. The sharp peak at 796 cm^{-1} and the weak band at 589 cm^{-1} are due to C-Cl and C-Br stretching vibrations of alkyl halides. The band assignments are tabulated in table 1.

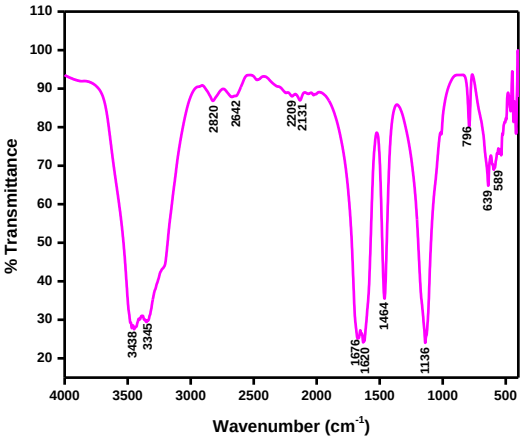

Fig. 4 FTIR spectrum of LVI

Table 1FTIR spectral band assignments of LVI

Wavenumber (cm^{-1})	Frequency Assignment
3438	O-H stretching
3345	N-H bending vibrations
2820	C-H bending vibration of alkanes
2642	O-H stretching
2209	C-N stretching vibration
2131	C-C stretching
1676	C=O stretching vibration
1620	N-H bending vibrations
1464	C-H bending vibration of alkanes
1136	C-N stretching vibration
796	C-Cl stretching vibrations of alkyl halides
639	C-H bending vibration of alkanes
589	C-Br stretching vibrations of alkyl halides

Optical studies

Nonlinear optical single crystals are mainly used in optical applications. The optical transmission range, transparency cut-off and the absorbance band are the most important optical parameters for laser frequency conversion applications. To find the transmission range of LVI, the optical transmission spectrum of the LVI for the wavelength range 190 - 1100 nm was recorded using Perkin Elmer Lambda UV-vis-NIR spectrometer. From the graph (Fig. 5), it is evident that the lower cut- off wavelength of the grown crystal is 248 nm and the crystal has wide transparency window between 200 nm and 1100 nm.

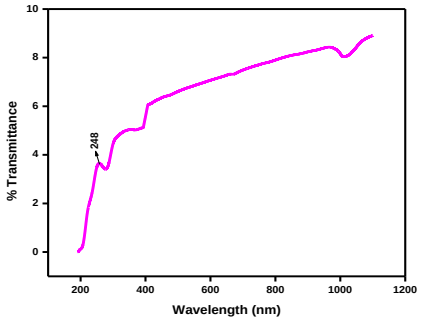

Fig. 5 UV-vis-NIR spectrum of LVI

Determination of the optical constants

The optical absorption coefficient (α) of the crystal was calculated using the formula

$$\alpha = \frac{2.303\log(1/T)}{t} \qquad (1)$$

wheret is the thickness of the crystal and T is the transmittance of the crystal. The optical band gap energy of the crystal can be found from Tauc's plot. The extrapolation of the linear part [11] of the Tauc's plot (Fig. 6) gives the optical band gap energy (E_g). The obtained value of E_g = 5.09 eV.

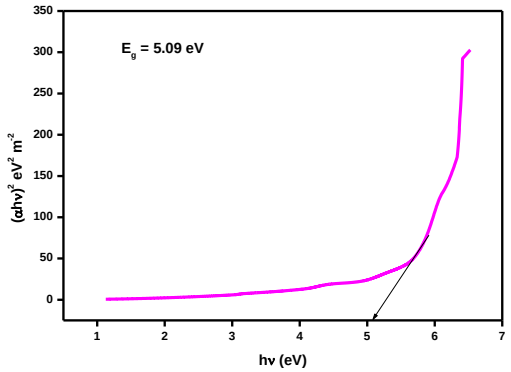

Fig. 6 Tauc Plot of LVI crystal $((\alpha h\nu)^2$vs photon energy (hν)

The extinction coefficient (K) to be obtained from the equation

$$K = \frac{\lambda\,\alpha}{4\pi} \quad (2)$$

where λ is the wavelength of the ultraviolet radiation. Fig.7 shows the variation in extinction coefficient (K) with the wavelength. The reflectance (R) in terms of absorption coefficient can be written as

$$R = 1 \pm \frac{\sqrt{1-exp\ (-\alpha t)+\exp(\alpha t)}}{1+\exp(-\alpha t)} (3)$$

The variation of reflectance as a function of wavelength is shown in Fig. 8. FromFig. 8 it is clear that the reflectance depends on the absorption coefficient. The internal efficiency of the material is also depending on the absorption coefficient. The refractive index of the crystal can be calculated from the reflectance value and the equation

$$n = -\frac{(R+1) \pm \sqrt{-3R^2+10R-3}}{2(R-1)} \quad (4)$$

where R is the reflectance and n is the refractive index. The refractive index of the material is found to be 0.38 at a wavelength of 1100 nm. The variation of refractive index with wavelength is shown in Fig. 9. From the plot, it is clear that the refractive index of the material decreases with an increase of wavelength [12]

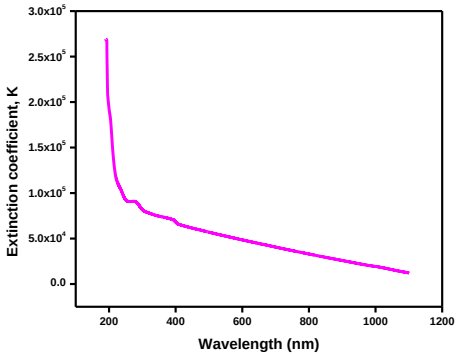

Fig. 7 Variation of extinction coefficient with wavelength

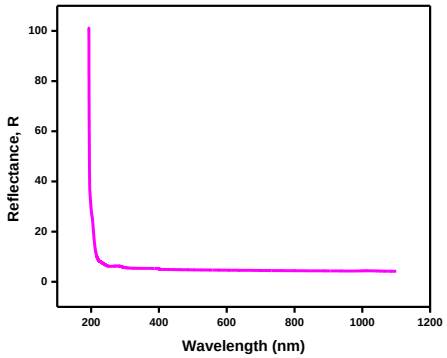

Fig. 8 Variation of reflectance with wavelength

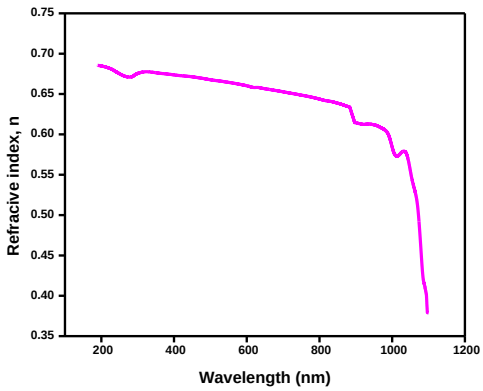

Fig. 9 Variation of refractive index with wavelength

The optical and frequency response of a material is mainly studied in terms of the optical conductivity (σ) which can be calculated using the following relation

$$\sigma_{op} = \frac{\alpha nc}{4\pi} (5)$$

where c is the velocity of light and n is refractive index. Optical conductivity is directly proportional to absorption coefficient and the refractive index of the material. Fig10 shows that the optical conductivity decreases with an increase of wavelength. The grown samples have a high and good magnitude of optical conductivity and it confirms that the grown materials have high photo response nature and also it suggests that the grown crystals are suitable for optoelectronic device applications and they are more prominent for device applications in information processing and optical computing [13].

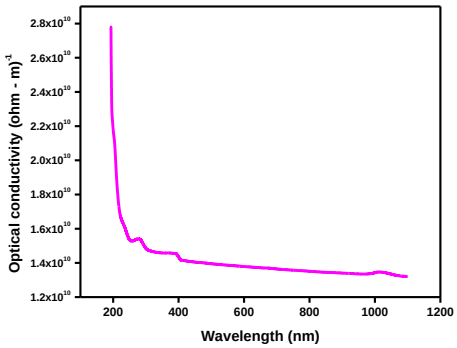

Fig. 10 Variation of optical conductivity with a wavelength

Non Linear optical (NLO) studies

The second harmonic generation behaviour of the powdered samples was determined using Kurtz and Perry powder technique. The standard potassium dihydrogen phosphate (KDP) powdered crystal sample was used as the reference. A Q-switched Nd-YAG laser beam of wavelength 1064 nm was used with the input power of 0.68 mJpulse of width 8 ns with the repletion rate of 10 Hz. The Powdered sample of grown crystals was tightly packed in a microcapillary tube and exposed to laser radiation. The output from the sample was monochromated to collect the intensity of 532 nm component and to eliminate the fundamental. Second harmonic radiation generated by randomly oriented microcrystals was focused by a lens and detected by a photomultiplier tube. The generation of the second harmonic was confirmed by the emission of green light. The SHG conversion efficiency of LVI crystal is 0.74 times as that of the standard KDP.

Mechanical studies

The mechanical properties such as hardness, yield strength and stiffness constant of crystals can be evaluated by Vickers hardness test. The hardness of a material depends on different parameters such as lattice energy, Debye temperature, the heat of formation and interatomic spacing. It is a measure of the material resistance to local deformation caused by scattering or by indentation [14].The microhardness studies of the grown LVI crystal were determined using the Vickers microhardness tester. The indentations were made on the polished crystal of LVI for loads of 25, 50 and 100 g. The indentation time was kept as 10 sec for all the loads. The Vickers microhardness number (H_v) was calculated using the relation $H_v = 1.8544\ P / d^2\ kg / mm^2$ where H_v is the Vickers microhardness number, P is the applied load in kg, d is the mean diagonal length of the indentation in mm and 1.8544 is a constant for the geometrical shape of diamond pyramidal indenter. The variation of hardness number with the applied load for LVI crystal is shown in the Fig.11. From the obtained data, it is observed that the hardness number increases with an increase of the applied load, showing the reverse indentation size effect (RISE). On further increase of the load beyond 100 g, cracks developed on the surface of the crystal. It may be due to the release of internal stress generated locally by indentation. When a low load is applied to the crystal, it seems that the crystal is hardened and it can withstand when high loads are applied until the crack is formed in the crystal.

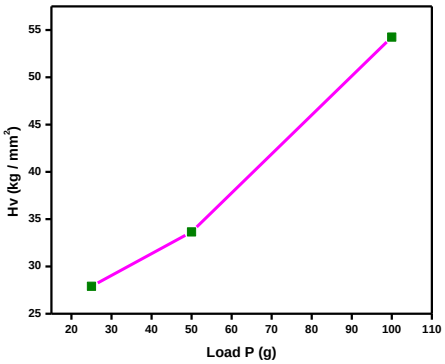

Fig. 11 Variation of the microhardness number Hv with the load

The relation connecting the applied load P and diagonal length d of the indenter is given by Meyer's law [15] where k is the material's constant and n is Meyer's index or work hardening coefficient. This is

calculated from the plot of log P vs log d (Fig. 12). Onitsch [16] pointed out that n lies between1 and 1.6 for moderately hard materials and it is more than 1.6 for soft materials. The value of n obtained for LVI is 4.97. Hence LVI belongs to a soft material category and is in agreement with the reverse indentation size effect (RISE). The yield strength is defined as the stress at which a predetermined amount of permanent deformation occurs and it is found using the relation yield strength (σ_v) = (Hv/3) where Hvis the hardness of the material. The load dependent on the yield strength of LVI crystal is presented in Fig.13. It is observed that yield strength increases with an increase in load and hence the grown crystal has relatively high mechanical strength. The elastic stiffness constant (C_{11}) [17] for different loads was calculated using Wooster's empirical formula $C_{11} = H_v^{7/4}$ and the variation of C_{11} with the load is depicted in Fig. 14. Stiffness constant is a measure of the ability of the material to resist deformation and it gives an idea about the tightness of bonding between neighbouring atoms. From Fig.14, it is observed that the stiffness constant increases with an increase of load and the high values of C_{11} indicate that the binding forces between the ions in the LVI crystal is strong.

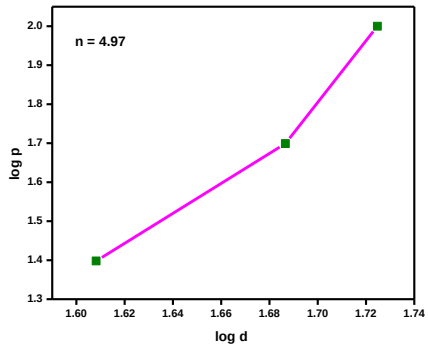

Fig. 12 Plot of log p vs log d

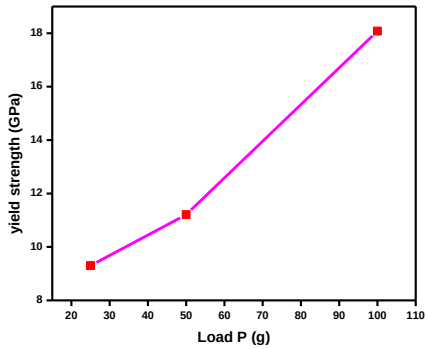

Fig13 Variation of yield strength with the load

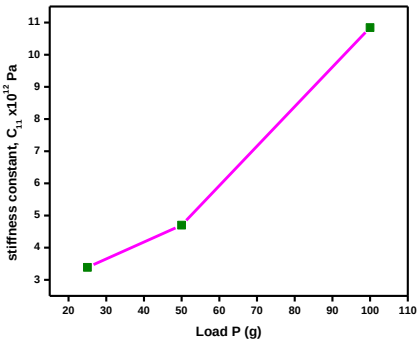

Fig 14 Variation of stiffness constant with the load

Fracture toughness

The resistance to fracture indicates the toughness of any material. Fracture toughness (K_c) determines how much fracture stress is applied under uniform loading and is an important parameter for the selection of materials for device applications where the load exceeds the limit or yield point. Fracture toughness provides the most reasonable estimation of the fracture resistance of brittle materials. The crack lengths (C) were measured

from centers of the indentation to the tip of the crack. $K_c = \frac{P}{\beta C^{3/2}}$ where β is a constant that depends upon the indentation geometry. For Vickers indenter, β is equal to 7. For the LVI crystal, the calculated $K_c$was 10.05 Kg $m^{-3/2}$.

Brittleness Index

Brittleness is an important property that affects the mechanical behavior of a material and gives an idea about the fracture induced in a material without any appreciable deformation. The value of brittleness index B is calculated using relation $B = H_v / K_c$. The calculated values of fracture toughness and hardness value for various loads are plotted in Fig.15. The graph shows the linear relationship between the parameters and the slope of this straight line gives the brittleness index of the sample. The brittleness index of LVI crystal is estimated as 0.563 x 10^3 $m^{-1/2}$. The low value of the brittleness index reveals the good dimensional stability of the grown crystal. The calculated stiffness constant C_{11}, yield strength $\sigma_v$and Vickers hardness values for different load range 25 - 100 g are provided in table 2.

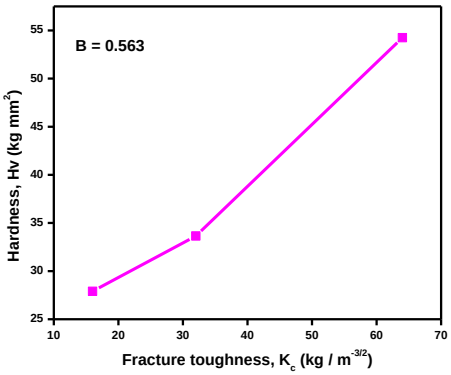

Fig 15 Plot of microhardness number with fracture toughness

Table 2 Values of microhardness parameters of LVI crystal

Load P (g)	H_v (kg mm^{-2})	Meyer's index n	σ_v (GPa)	C_{11} x 10^{12} (Pa)
25	27.90	4.97	9.30	3.38
50	33.65	4.97	11.21	4.70
100	54.25	4.97	18.08	10.84

Hays-Kendall (HK) approach

The dependence of indentation size (d) on the applied indentation test load (P) are examined by Hays-Kendall approach by the relation $P = W + A_1 d^2$ where W is the minimum load to initiate plastic (permanent) deformation in grams and A_1 is the load independent constant. These two values have been estimated by plotting a graph of P vs.d^2 for the loads 25-100 g as shown in Fig.16. As the grown crystal exhibits reverse indentation size effect, the estimated value W is found to be negative [18]. The corrected hardness value H_{HK} has been determined using the relation, H_{HK}= 1854.4 A_1. The values of W and H_{HK} are - 81.54 g and 114.04 g/ μm^2 respectively for LVI crystal.

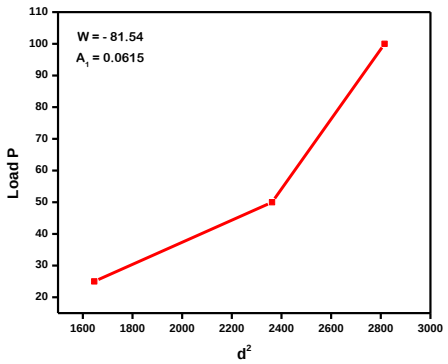

Fig. 16 Plot of load P vs d^2

Surface laser damage threshold

Laser damage threshold property of the grown crystal was studied to quantify its capacity to withstand the high power lasers. The cut and polished LVI crystal were mounted on the crystal holder in the path of Q-switched Nd:YAG laser beam of wavelength 1064 nm. The crystal was exposed to the laser beam for a time period of 6ns. The spot size of the laser beam was kept as 1 mm. The observations were made at different energies. As the energy increased, a dot like a mark started appearing on the crystal even for a short duration of time. The surface damage threshold of the grown crystal was calculated using the power density expression. The quantified laser damage threshold value of LVI crystal is 11 GW / cm^2. This threshold value of the grown crystal is compared with that of KDP and Urea [19]. The LDT values are tabulated in Table 3.

Table 3 Comparison of LDT value of LVI with KDP and Urea

Compound	Laser damage threshold (GW/cm^2)
KDP	0.20
Urea	1.50
LVI (present work)	11

Thermal analysis

The thermogravimetric analysis (TGA) and differential thermal analysis (DTA) were carried out in the temperature range of 40 - 700 ^oCat the heating rate of 20 ^oC / min in the nitrogen atmosphere, using Perkin Elmer Diamond TG / DTA thermal analyzer. Crystal weighing about 10.558 mg was used for this study. From the TG curve (Fig. 17) it is noticed that there is a maximum weight loss in the temperature range 203 ^oC - 366 ^oC and hence the sample is observed to be thermally stable and suitable for device applications. From the DTA curve, it is observed that the LVI crystal shows the first endothermic peak at 226 ^oC and the second endothermic peak at 359 ^oC which corresponds to the decomposition point of the sample. The broad exothermic peak beyond 369 ^oC indicates the liberation of the compounds as gaseous products such as NH_2 and CO_2 etc. and the decomposition is completed beyond 695 ^oC.

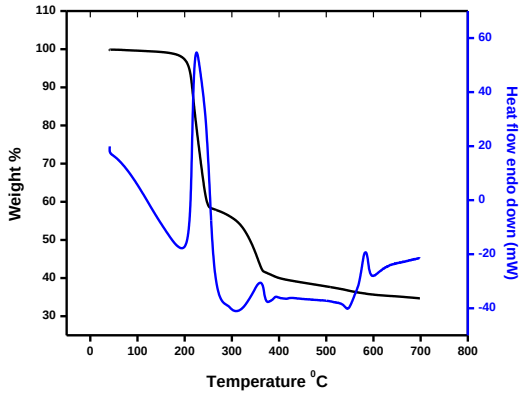

Fig. 17 TG/DTA curves for LVI

Scanning electron microscopy (SEM)

The SEM micrograph of the title crystal is shown in Fig.18. From the figure, it is noticed that the LVI complex exhibits the cylindrical shape-like structure with an average particle size of 1 - 10 µm. This may be due to solvent inclusions, which is generally observed in solution grown crystals.

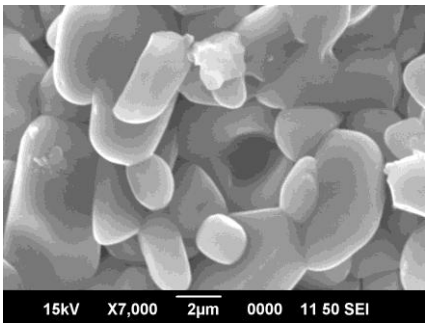

Fig. 18 SEM image of as-grown LVI

Fluorescence studies

Fluorescence property is used to determine the crystalline quality as well as its exciton fine structure. The fluorescence emission spectra for LVI crystal sample was recorded in the range from 280 to 700 nm. The sharp band at 530 nm is observed in the emission spectrum. The fluorescence spectrum of LVI crystals is shown in Fig.19. The emission was assigned to the electronic transition from π* antibonding molecular orbital to π bonding molecular orbital of the grown crystal. The higherintensity ratio indicates purity and perfect crystallinity ofthe title compound. Hence, the grown crystal is suitable foroptoelectronic laser devices.

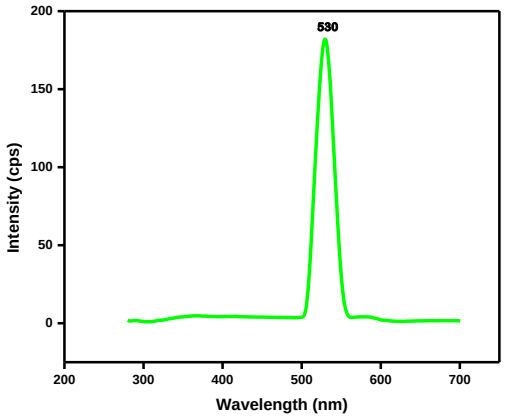

Fig. 19 Fluorescence spectrum of LVI crystal

IV. Conclusion

Thesingle crystal of L-Valine imidazole was successfully grown by a slow evaporation technique. Single X-ray diffraction study confirms the lattice parameter values of the grown crystal and it is in good agreement with the reported values. FTIR studies confirm the presence of L-Valine and imidazole ions in the crystal. Optical studies were carried out for the grown crystal and the crystal has wide transparency window between 190 nm and 1100 nm. Various optical constants were calculated and the optical band gap energy of the crystal is found to be 5.09 eV. The extinction coefficient (K) and reflectance depend on the photon energy. The refractive index of the material is found to be 0.38 at a wavelength of 1100 nm. Optical conductivity is calculated from the UV- vis absorbance value and the grown crystal possesses high optical conductivity. The SHG efficiency of the grown LVI crystal is 0.74 times as that of the KDP crystal and hence LVI crystal is suitable for device fabrication. Vickers hardness numbers were calculated for LVI crystal by the application of load and the hardness numbers were found to increase with an increase in load. It was observed that the hardness increases with increasing load, termed as reverse ISE. The value of Meyer's index n turned to be greater than 1.6 and thus LVI falls in the soft material category. The calculation of the stiffness constant reveals that the binding force between the ions is quite strong. The fracture toughness of the material is found to be 10.05 Kg $m^{-3/2}$. The value of B is calculated as 0.563 x 10^3 $m^{-1/2}$. The hardness measurements may be useful in indicating the order of magnitude to be expected for the elastic constant in a new material. The laser damage threshold value of LVI crystal is 11 GW / cm^2 which is greater than the standard KDP material. TG/DTA analysis techniques confirm the melting point and decomposition temperature of the crystal.The SEM micrograph of LVI indicates that the crystal exhibits the cylindrical shape - like structure with an average particle size of1-10 μm. Fluorescence spectrum shows that the sharp emission peak occurs at 530 nm. The results strongly suggest that the material could be used in optical device fabrication.

References

[1] Zhang, C, Li, CZ, Cong, H, Wang, J, Zhang, H &Boughton, RI 2010, 'Crystal growth and thermal properties of single crystal monoclinic NdCOB (NdCa4O(BO3)3)', Journal of Alloys and Compounds, vol. 507, pp. 335–340.

[2] Arjunan, S, Bhaskaran, A, Mohan Kumar, R, Mohan, R &Jayavel, R 2010, 'Effect of rare-earth dopants on the growth and structural, optical, electrical and mechanical properties of L-arginine phosphate single crystals', Journal of Alloys and Compounds, vol. 506, pp. 784–787.

[3] Uthrakumar, R, Vesta, C, Bhagavannarayana, G, Robert R & Jerome Das, S 2011, 'Optical, crystalline perfection and mechanical studies on unidirectional grown bis(thiourea) cadmium zinc chloride single crystal', Journal of Alloys and Compounds, vol. 509, pp. 2343–2347.

[4] Mohd.Shakir, Riscob, B, Maurya, KK, Ganesh, V, Wahab, MA &Bhagavannarayana, G 2010, 'Unidirectional growth of L-

asparagine monohydrate single crystal: First time observation of NLO nature and other studies of crystalline perfection, optical, mechanical and dielectric properties', Journal of Crystal Growth, vol. 312, pp. 3171-3177.

[5] Dhanaraj, PV, Rajesh, NP &Bhagavannarayana, G 2010, 'Synthesis, crystal growth and characterization of an organic NLO material: Bis(2-aminopyridinium) maleate', Physica B Condensed Matter, vol. 405, pp. 3441–3445.
[6] Rao, ST 1969, 'Crystal structure of L-valine hydrochloride monohydrate', Z. Kristallogr., vol. 128, pp. 339-351.
[7] Parthasarathy, R 1966, 'The structure of L-valine hydrochloride', ActaCryst., vol. 21, pp. 422.
[8] Pandiarajan, S, Sridhar, B &Rajaram, RK 2001, 'L-valine L-valinium perchlorate monohydrate', ActaCryst., vol. E57, pp. 0466.
[9] Srinivasan, N, Rajaram, RK &Jebaraj, DD 1997, 'Crystal structure of hexaammoniumdicosaoxodiperoxoheptamolybdate (VI) - water (1/6)', Z. Kristallogr., vol. 212, pp. 311-312.
[10] Lipson, H & Steeple, H 1970, Interpretation of X-Ray Powder Diffraction patterns, fifth ed. Macmillan, New York.
[11] Chawla, AK, Kaur, D & Chandra, R 2007, Structural and optical characterization of ZnOnanocrystalline films deposited by sputtering'', Optical Mater. vol. 29, pp. 995-998.
[12] Ilakiya, D, JothiMani, R &Muthuselvi, A 2017, 'Linear Optical Constants of Succinic Acid Single crystals (SA) **',** International Journal of Science, Engineering and Management (IJSEM), vol. 2, Issue 12, pp. 44-46.
[13] Pal Tanusri&KarTanusree 2005, 'Studies of microhardness anisotropy and Young's modulus of nonlinear optical crystal L-arginine hydrochlorobromo monohydrate', Materials Letter, vol.59, pp. 1400-1404.
[14] Mott, W 1956, Micro Indentation Hardness Testing, Butterworths, London,
[15] Meyer, E &Ver, Z 1908, 'Contribution to the knowledge of Hardness and Hardness testing', Dtsch. Ing., vol. 52, pp. 645-654.
[16] Onitsch, EM 1950, 'The present status of testing the hardness of the materials', Mikro-scopie, vol. 95, pp. 12.
[17] Wooster, WA 1953, 'Physical properties and atomic arrangements in crystals', Rep.Prog. Phys. vol.16, pp. 62.
[18] Sangwal, K, Hordyjewicz, M and Surowska, B 2002, "Microindentationhardeness of SrLaAlO4 and SrLaGaO4 single crystals", J. Optoelectron. Adv. Mater. Vol. 4, No. 4, pp. 875-882.
[19] Martin BrittoDhas, SA &Natarajan, S 2007, 'Growth and characterization of L-prolinium tartrate - A new organic NLO material', Crystal Research Technology, vol. 42, pp. 471-476

IOSR Journal of Applied Physics (IOSR-JAP) is UGC approved Journal with Sl. No. 5010, Journal no. 49054.

K. Lilly Mary Eucharista 'Synthesis, Growth, Linear and Nonlinear Optical Properties Of L-Valine Imidazole: An Organic Nonlinear Optical Single Crystal" IOSR Journal of Applied Physics (IOSR-JAP), vol. 10, no. 5, 2018, pp. 15-25.